Supporting Information for: **Ion mobility spectrometry nuisance alarm threshold analysis for illicit narcotics based on environmental background and a ROC-curve approach**

Thomas P. Forbes* and Marcela Najarro

National Institute of Standards and Technology, Materials Measurement Science Division, Gaithersburg, MD, USA

* Corresponding author: *E-mail: thomas.forbes@nist.gov*

TABLE OF CONTENTS

Additional Data Processing Details. The calibrants, trinitrotoluene (TNT, negative mode calibrant) and cocaine (positive mode calibrant) were introduced through PTFE-coated fiberglass calibration swabs (Calibration Traps-CT1319, DSA Detection, LLC, Boston, MA, USA) and the drift time corrected by a calibration factor based on the calibrants' measured and specified drift times. Following an initial "learning" period during the first few months with one or two calibrations per day, the field instrument consistently recorded two calibration files per day, one in the morning and one in the afternoon. IMS data were collected during the sampling time for each experiment and consisted of 120 individual scans (spectra) in Mode 1 and 165 in Mode 2. Representative IMS spectra for the illicit narcotics investigated here are displayed in Figure 1 of the article. Peaks were identified from the processed IMS spectra, examples displayed Figure S-1, and batch processed using a MATLAB-based code developed in-house (MATLAB R2015a, Mathworks, Inc., Natick, MA, USA).

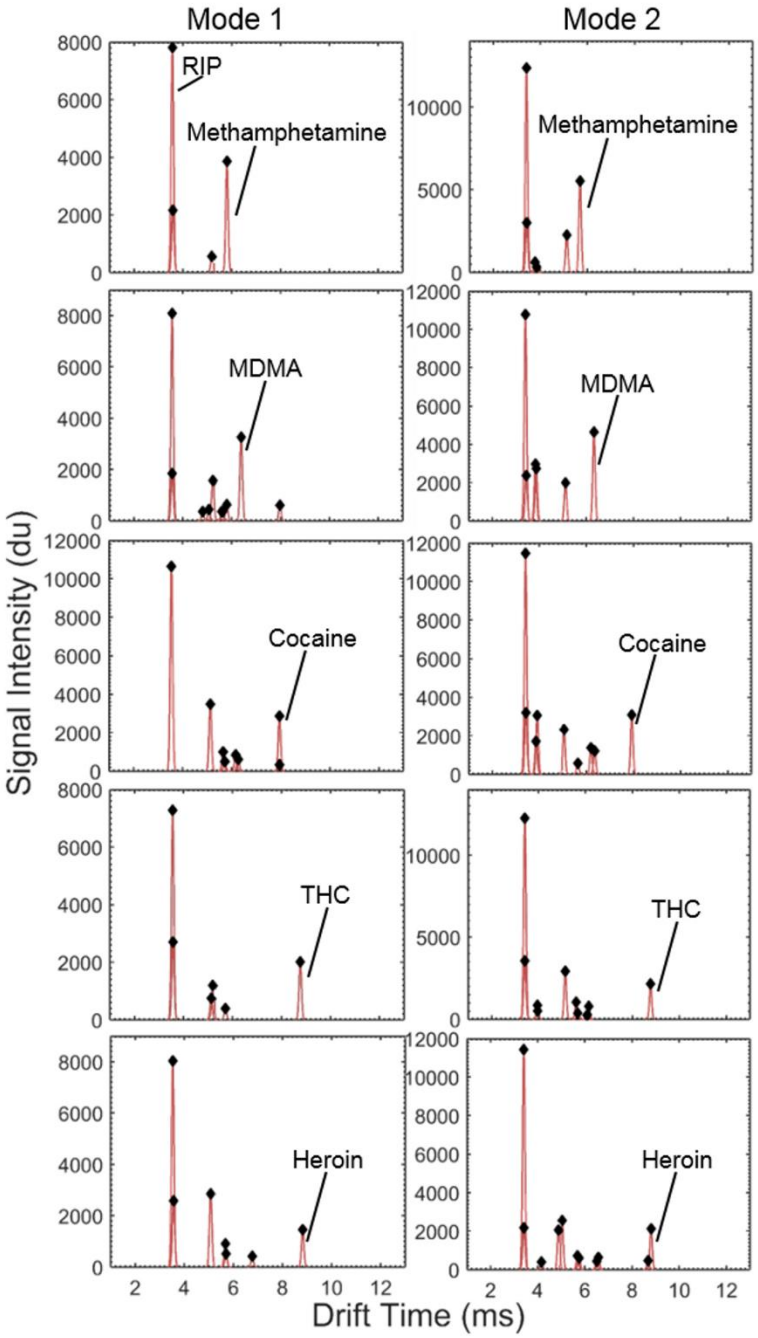

Figure S-1. Firmware processed peak determinations for adjusted amplitude at maximum slope (with respect to scan number) from representative raw IMS spectra for select illicit narcotics in Mode 1 (methamphetamine: 10 ng, MDMA: 10 ng, cocaine: 10 ng, THC: 10 ng, heroin: 200 ng) and Mode 2 (methamphetamine: 5 ng, MDMA: 15 ng, cocaine: 5 ng, THC: 5 ng, heroin: 25 ng).

Deployed Instrument Calibration Monitoring

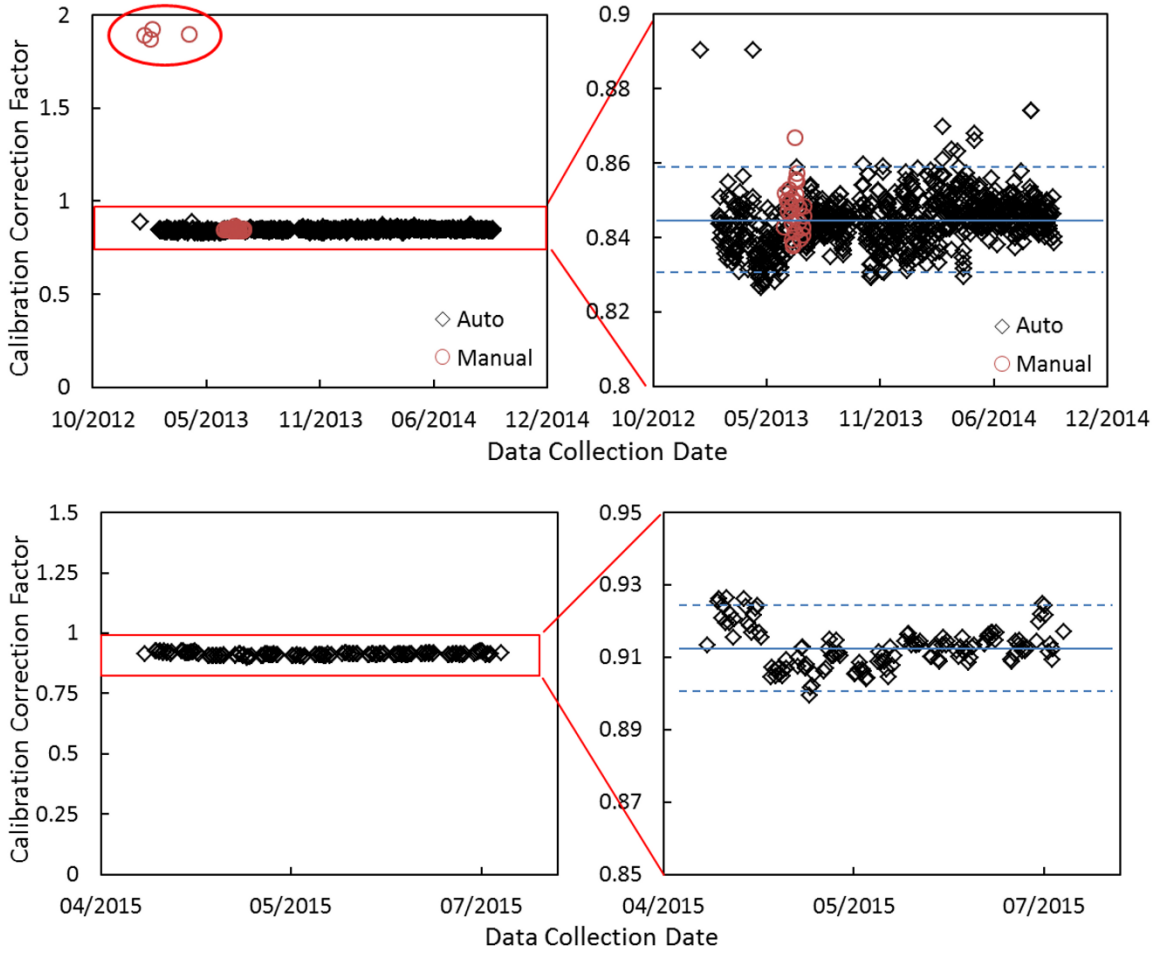

Figure S-2. Calibration correction factor as a function of time in (top) Mode 1 and (bottom) Mode 2 for the deployed IMS instrument. Zoomed insets demonstrate the average (solid line) and 95% confidence intervals (dashed lines). Manual calibration outliers near 1.9 in early 2013 (circled in red) were excluded in the average calculations.

Environmental Background – True Negatives

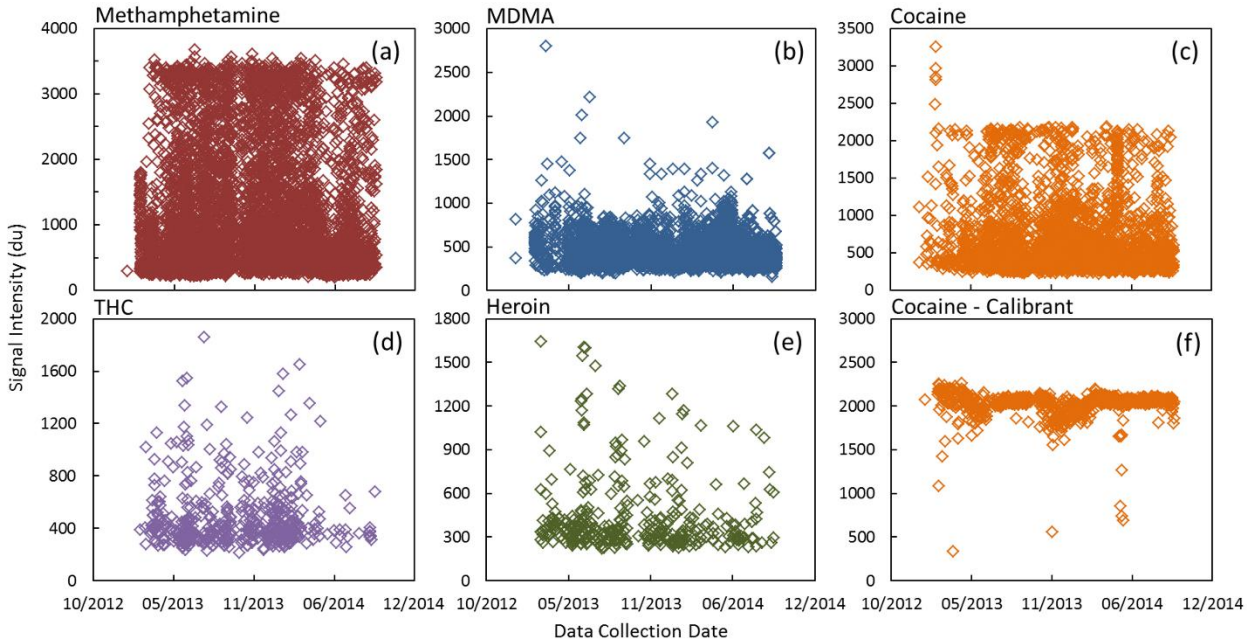

Figure S-3. (a) – (e) Intensity data from the deployed IMS instrument in Mode 1 across a 21-month period (18,504 total files/samples). Drift times measured with a ± 0.05 ms window were utilized here. (f) Intensity data for cocaine from the calibration files across the 21-month period (739 calibrations).

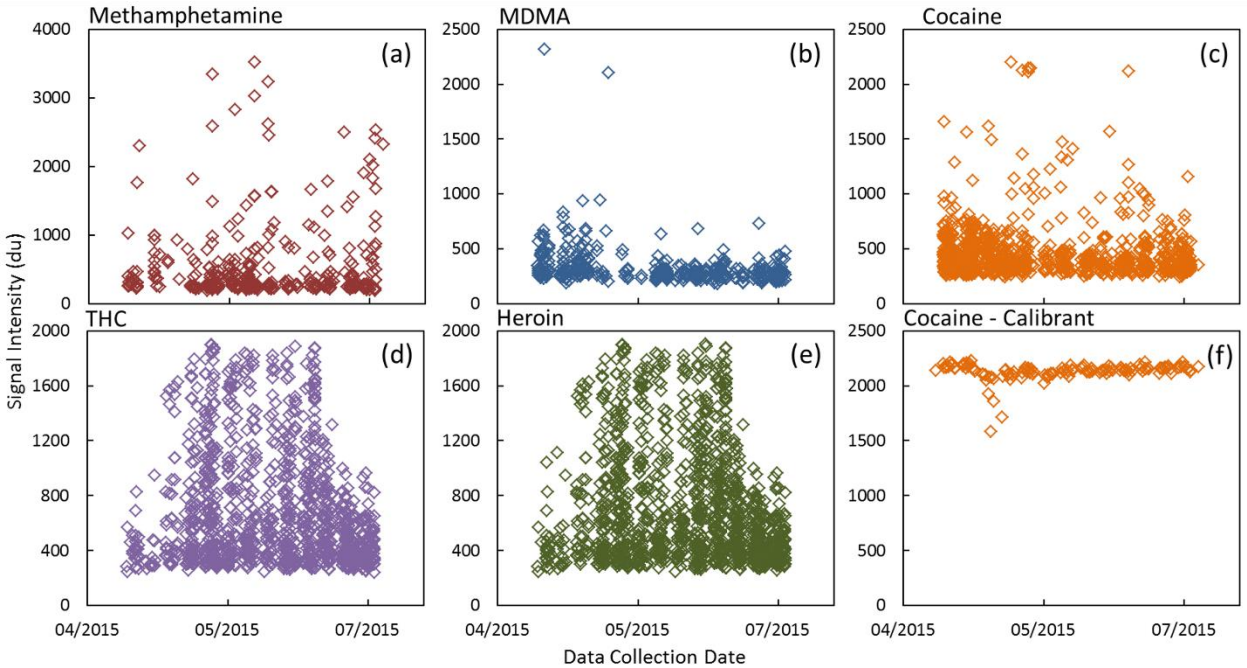

Figure S-4. (a) – (e) Intensity data from the deployed IMS instrument in Mode 2 across a 3-month period (3,293 total files/samples). Drift times measured with a ± 0.05 ms window were utilized here. (f) Intensity data for cocaine from the calibration files across the 3-month period (129 calibrations).

Target Response – True Positives

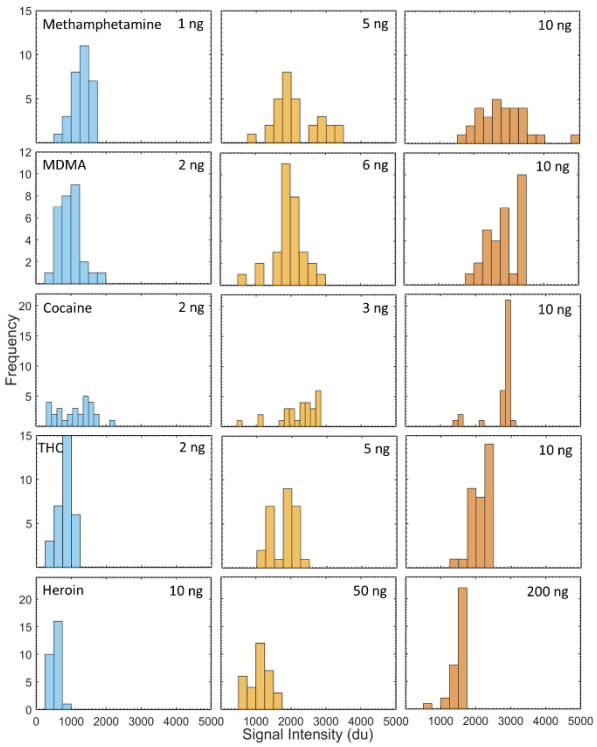

Figure S-5. Frequency histograms of analyte intensity data from the laboratory IMS instrument in operating Mode 1 for approximately 30 replicates at each of three different mass loadings.

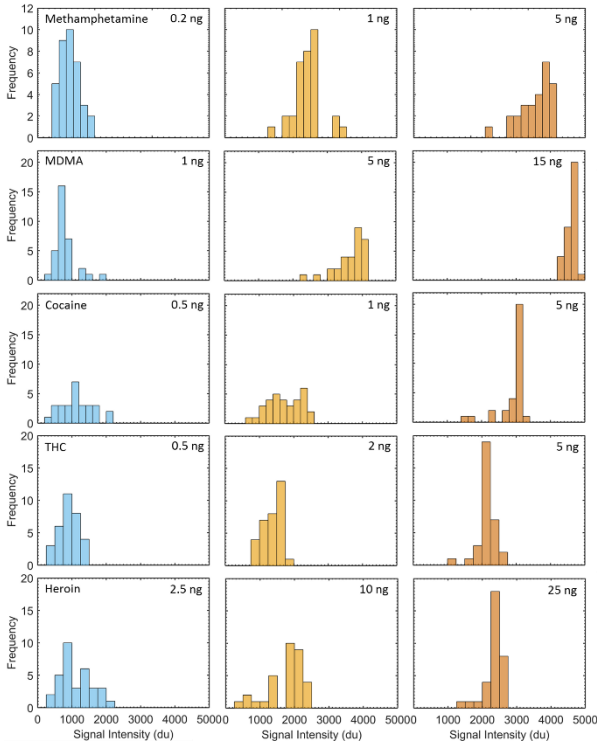

Figure S-6. Frequency histograms of analyte intensity data from the laboratory IMS instrument in operating Mode 2 for approximately 30 replicates at three different mass loadings.

Representative IMS Spectra as a Function of Scan Number

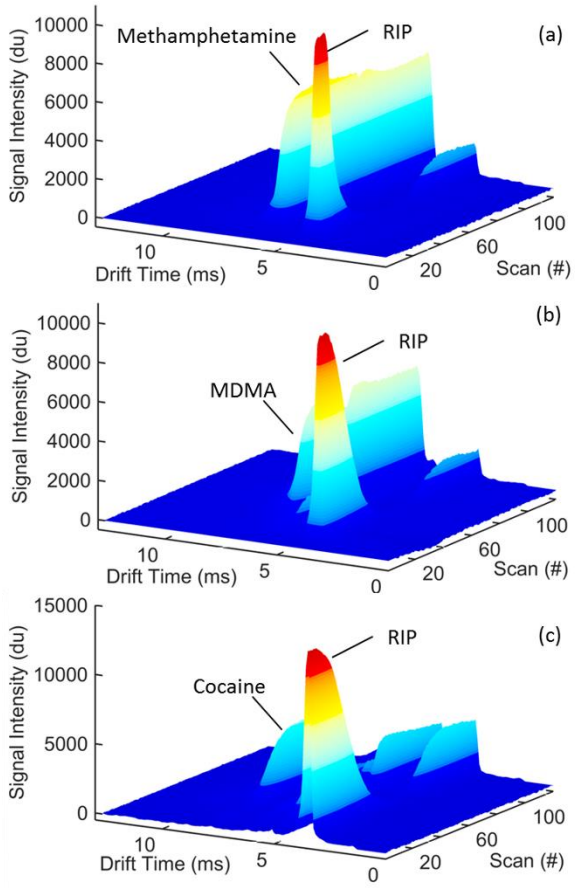

Figure S-7. Representative IMS spectra for (a) 10 ng methamphetamine, (b) 10 ng MDMA, and (c) 10 ng cocaine displaying signal as a function of drift time and scan number in Mode 1.

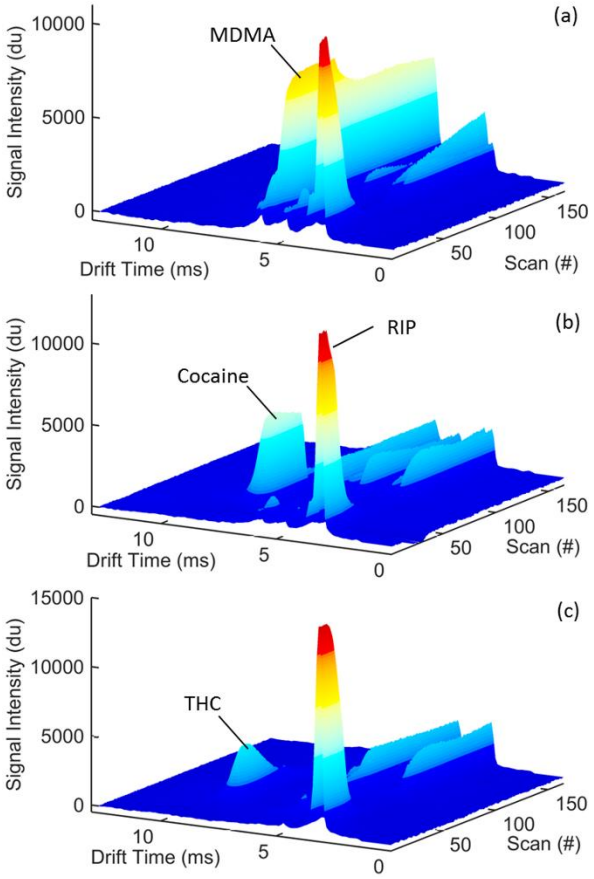

Figure S-8. Representative IMS spectra for (a) 15 ng MDMA, (b) 5 ng cocaine, and (c) 5 ng THC displaying signal as a function of drift time and scan number in operating Mode 2.

Background and Target Distributions

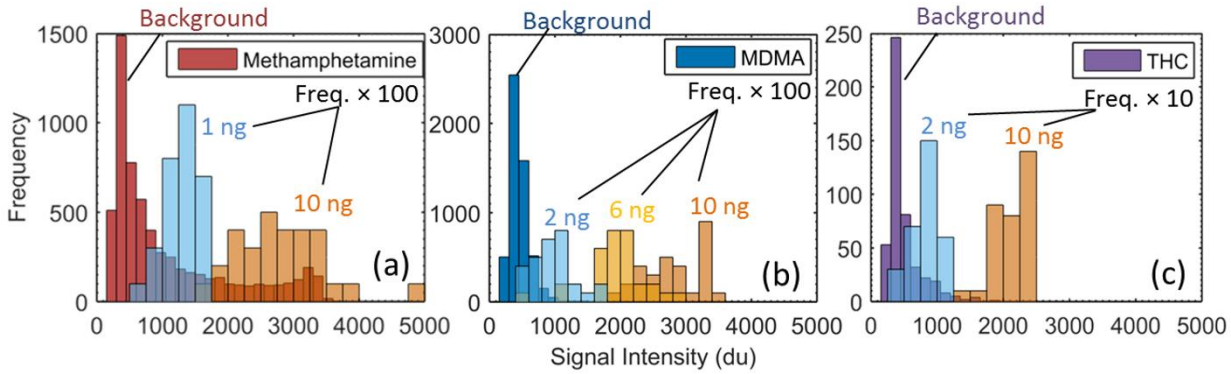

Figure S-9. (a) – (c) Overlaid frequency histograms of background and target narcotic intensity data in operating Mode 1. Target narcotic frequencies were multiplied by factors as specified in the figure for appropriate visualization of the data.

AUC as a Function of Drift Time Window. The size of the drift time window was investigated with respect to each compound and mass loading. The area under a ROC curve (AUC) was used as a measure of a given set of experimental conditions to discriminate between target detection and environmental background, as well as compare between sets of conditions; an AUC = 0.5 signifies no discrimination and AUC = 1.0 represents perfect discrimination (100% TPR and 0% FPR). Drift time windows of ± (0.025, 0.035, 0.05, 0.065, 0.075) ms for each target analyte and mass were investigated, demonstrating a number of trends in AUC (Figure S-10 and S-12). These trends varied significantly from analyte to analyte and between modes of operation; however, they remained relatively self-similar across mass loadings of each analyte.

For Mode 1 conditions, a ± 0.025 ms window around the methamphetamine drift time, fewer background peaks were identified, pushing the ROC curves toward a lower FPR and increasing the AUC (Figures S8 and S9). However, increasing that window to ± 0.035 ms, resulted in more collected background measurements across the intensity range contributing to the FPR and decreasing the overall AUC. That trend then reversed, demonstrating increased AUC with further increases in the window size from ± 0.05 ms to ± 0.065 ms to ± 0.075 ms. In this range, the increase in the background measurements falling within the methamphetamine window were skewed heavily to the lower signal intensity regime. This phenomenon resulted in an overall increase in the number of background methamphetamine peaks; however, the majority of the peaks were below the alarm threshold, leading again to a decrease in the FPR and increase in AUC. From the distribution of MDMA samples, changing the drift time window had little effect on the ROC curves and AUC. Cocaine exhibited a continuous increase in AUC for increasing drift time window. Similar to methamphetamine, increases to the widow size resulted in proportionally more low signal intensity peaks falling within the cocaine window. Again, this manifested as a shift in the ROC curves to the left – toward improved discrimination – and led to increased AUC. THC and heroin revealed similar results; however, there were some differences in the trends due to the proximity of their drift times and window overlap for window sizes of ± 0.05 ms and greater, 8.7736 ms and 8.8557 ms, respectively.

As with Mode 1 operating conditions, the drift time window specifying each narcotic was varied and the discrimination between target and background evaluated in Mode 2. The change in IMS system parameters for Mode 2 resulted in differences in the distributions of the environmental background, which in turn resulted in changes in the trends observed for the AUC of each narcotic as a function of drift time window (Figure S10 and S11). The target narcotics again demonstrated self-similar behavior across the mass loadings investigated. Increasing the drift time window for the identification/detection of methamphetamine (Figure S11) and MDMA both led to a decrease in the AUC and discrimination potential. These trends were a direct result of increased high and low intensity environmental background within these windows, believed to be a function of the increased desorption temperature and sampling time. Higher mass loading for MDMA (and, in general, most cases) pushed the target signal well beyond the background, resulting in little dependence between AUC/discrimination potential and the window size. Cocaine demonstrated a similar relationship, however, proportionally more low intensity background peaks were measured, reducing the FPR and increasing the AUC with window size. Tight drift time windows resulted in relatively high level of discrimination between THC and background. As the window broadened, initially more high intensity background peaks reduced discrimination/increasing the FPR. This trend reversed as the largest windows encompassed the high frequency areas of low intensity background, decreasing the FPR (Figure S11). Finally, heroin demonstrated similar trends to those observed in Mode 1, as the window increased, greater levels of low intensity background peaks were included, decreasing the overall FPR for a given threshold, and improving discrimination.

In general, when the window size adjustment (either larger or smaller) led to an increase in the number of low intensity "negative" measurements (background peaks), the discrimination and increasing the AUC. However, the opposite applied when the number of low intensity negative measurements decreased. Alternatively, when the adjustment led to an increase in the number of high intensity background peaks, the FPR increased, decreasing the AUC (Figures S-10 – S-13). The distribution and intensity of the environmental background signals dictated the optimal window size for each narcotic,

reinforcing the need for each threat arena and application to assess their particular background distribution.

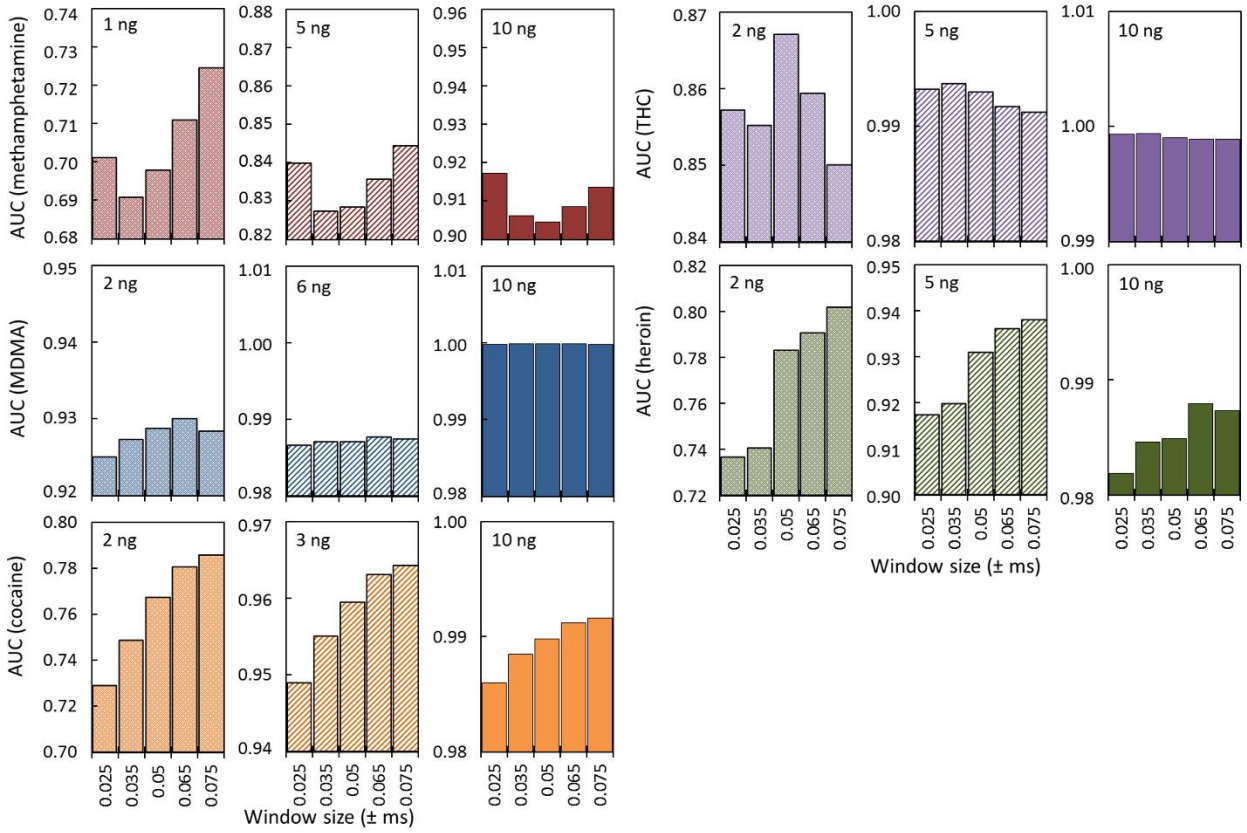

Figure S-10. Area under ROC curves as a function of drift time window for each target narcotic at three mass loading levels (methamphetamine: (1, 5, 10) ng, MDMA: (2, 6, 10) ng, cocaine: (2, 3, 10) ng, THC: (2, 5, 10) ng, and heroin: (10, 50, 200) ng) for IMS operating in Mode 1.

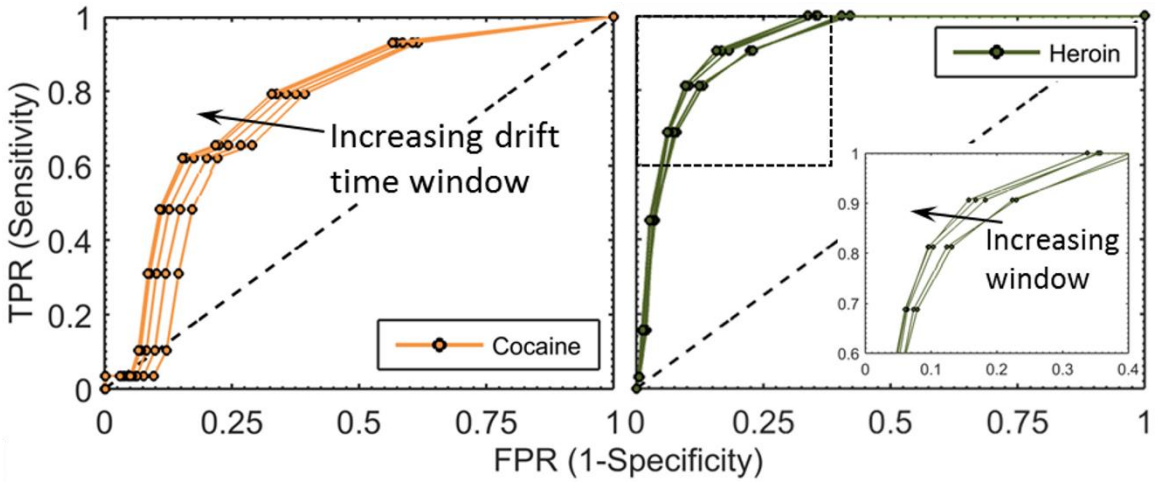

Figure S-11. ROC curves as a function of increasing drift time window for IMS operation in Mode 1 of 2 ng cocaine and 50 ng heroin. Nuisance/alarm thresholds were varied from 0 du to 4000 du in 200 du increments.

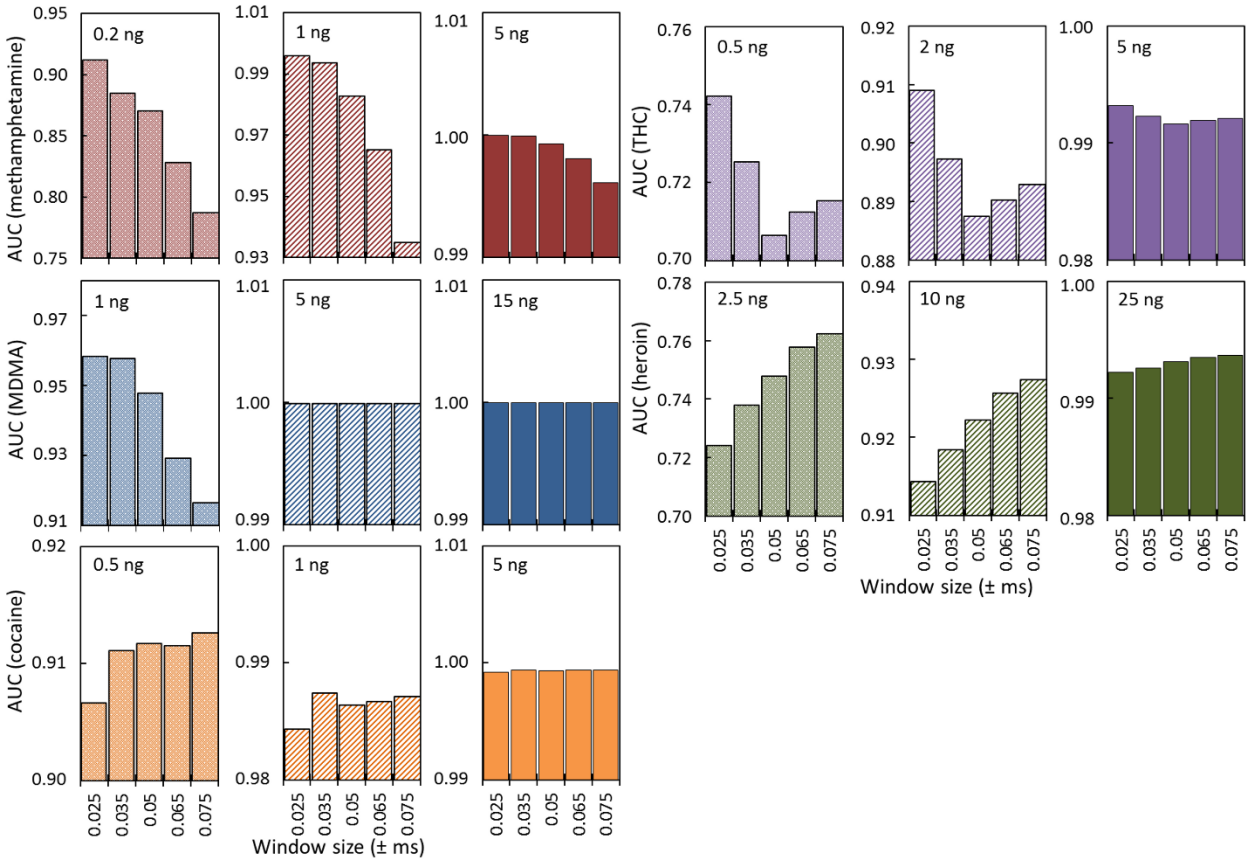

Figure S-12. Area under ROC curves as a function of drift time window for each target narcotic at three mass loading levels (methamphetamine: (0.2, 1, 5) ng, MDMA: (1, 5, 15) ng, cocaine: (0.5, 1, 5) ng, THC: (0.5, 2, 5) ng, heroin: (2.5, 10, 25) ng) for IMS operating in Mode 2.

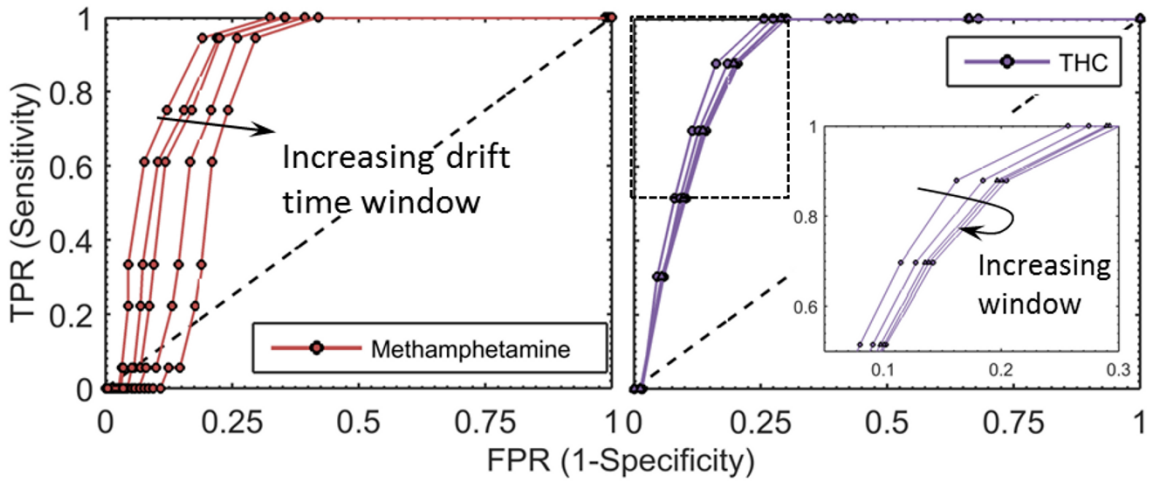

Figure S-13. ROC curves as a function of increasing drift time window for IMS operation in Mode 2 of 200 pg methamphetamine and 2 ng THC. Nuisance/alarm thresholds were varied from 0 du to 4000 du in 200 du increments. THC inset arrow demonstrates the decreasing-then-increasing AUC as the drift time window increases as demonstrated in Figure S-10.